Fatigue Crack Growth and Closure in a SiC_p-Reinforced Aluminum Composite

C. P. YOU and J. E. ALLISON
Scientific Research Lab., Ford Motor Co., 20000 Rotunda, Dearborn, MI 48121, USA

ABSTRACT

The fatigue crack growth behavior of a high-strength aluminum alloy, 2124, reinforced with 20% SiC_p was investigated over a range of aging conditions. Of particular interest were crack/microstructure interactions at various levels of applied ΔK. It was found that as ΔK levels increased from near-threshold to overload, there was a gradual transition of fracture mode resulting in a high incidence of reinforcement particle/matrix decohesion at low ΔK and a predominance of particle cracking at higher ΔK levels. Crack tip shielding due to different mechanisms was also investigated. Possible contributions due to asperity (surface-roughness)-, oxide-, and plasticity-induced closure are described.

KEYWORDS

Fatigue crack growth; closure; metal matrix composites; aluminum alloys.

INTRODUCTION

Metal matrix composites have been shown to offer substantial improvements in certain physical and mechanical properties over their monolithic counterparts. However, these improvements are generally attained at the expense of fracture-related properties. Recent work has shown that microstructural inhomogeneities introduced during the processing of these composites can be responsible for the initiation of premature failure. This has been found to be the case for both monotonically loaded tensile specimens (You et al., 1987[1]) as well as smooth bar fatigue specimens (VanDePolder and Jones, 1988).

With this in mind, an investigation was carried out to determine fatigue crack growth behavior from a pre-existing defect or notch. Of specific interest was the role of composite microstructure in determining fatigue crack growth behavior and fatigue crack paths. The influence of aging on fatigue crack growth behavior was examined, and compared with that

reported for monolithic aluminum alloys. Crack closure behavior was also examined for these composites, as a function both of aging as well as applied ΔK.

EXPERIMENTAL PROCEDURE

The material studied was a high strength 2124 aluminum alloy (Al-4Cu-2Mg[1]) reinforced with 20% SiC particles. This composite was obtained from DWA Composite Specialties (Chatsworth, CA) in the form of extruded bar (reduction ratio = 20:1). Processing of the composite was by a powder metallurgy (PM) route, involving blending of aluminum powder and SiC particles, compaction, consolidation at temperatures above the solidus, and hot extrusion.

Typical microstructures for this material are shown in Fig. 1. Quantitative metallographic analyses indicated a large range of both reinforcement particle size and spacing. Average values for both particle size and spacing were on the order of 5 μm. Back-scattered electron microscopy showed an additional intermetallic phase (present to about 4 v/o) which was probably the result of super-solidus consolidation temperatures.

The thermo-mechanical treatment used in sample preparation consisted of solution heat treatment at 495°C for 4 hours, followed by an ice water quench, and subsequent aging. In order to minimize residual stress effects on fatigue crack growth, the plates were stretched after quenching to a plastic strain of 1%. Aging treatments included natural aging for 48 hours at room temperature (T4 condition) and artificial aging at 190°C for 3 hours (underaged condition), 8 hours (peakaged condition), and 48 hours (overaged condition).

Fatigue crack growth tests were conducted on compact tension (CT) specimens machined in the L-T orientation with W = 40 mm, B = 8mm. An automated test control and data acquisition system was used to perform the fatigue testing. All testing was carried out at an R ratio of 0.1 in laboratory air, with relative humidity levels in the range of 40-50%. Closure loads were determined using global compliance measurements obtained from a clip-gauge located at the specimen notch mouth. Closure was defined at the 1% deviation level using the differential compliance technique.

Testing was carried out in general accordance with ASTM E647 recommended practices, with the exception that the precrack lengths used were significantly longer than the recommended minimum. These lengths were dictated by results of constant K_{max} tests (You et al., 1988). Load shedding procedures were used to determine crack growth rates in the range 10^{-5} to 10^{-9} mm/cycle (starting K_{max} = 8 MPam$^{1/2}$). When crack growth rates of less than $1x10^{-8}$ were reached, constant load testing was initiated at a stress intensity level of 6 MPam$^{1/2}$. This provided substantial overlap

[1] Although 2124 typically contains 0.6% Mn, the base alloy of this composite has no manganese. Manganese is usually present as a grain refining agent, and in PM processed aluminum composites substantial grain growth is not expected.

between the two test procedures, and allowed testing to be continued to failure.

Fractography and crack profile examination were conducted on a JEOL 840 scanning electron microscope.

RESULTS AND DISCUSSION

The results of fatigue crack growth tests over a wide range of growth rates (down to 10^{-9} mm/cycle) are shown in Fig. 2 for all four conditions studied. No significant differences in fatigue crack growth behavior for the different aging conditions were observed at growth rates above about 10^{-5} mm/cycle. At near-threshold growth rates, however, small differences existed as a function of aging, and threshold ΔK values varied from 3.5 to 4 MPam$^{1/2}$.

The well-documented trend in monolithic aluminum alloys of increased aging leading to lower ΔK_{th} (Carter et al., 1984; Zedalis and Fine, 1982; Zaiken and Ritchie, 1985) appears to be also borne out in these reinforced materials. However, the magnitude of the difference is much smaller than that reported for monolithic alloys. In those alloys, the change in slip behavior from planar slip in the underaged material to wavy slip in the overaged condition results in substantially higher closure levels in the underaged condition, due to higher levels of asperity-induced closure. A review of the literature on monolithic aluminum alloys, however, indicates that grain size can have a large effect on the above behavior (Bretz et al., 1984; Vasudevan and Bretz, 1984). Material processed by ingot metallurgy behaves in much the manner described above; powder metallurgy processed material, on the other hand, typically has finer grain sizes and differences in closure levels as a result of aging are therefore substantially reduced, at least in Al-Zn-Cu-Mg (7xxx) systems. The current results conform to those observed for monolithic PM alloys. Work is currently underway to examine the crack growth behavior of 2124 unreinforced matrix material processed in the same fashion as the composite. These results will indicate if the lack of significant effect of aging on fatigue crack growth behavior is merely due to the fine grain size of the composite or if a further effect of reinforcement is present.

Closure Mechanisms. The closure stress intensity levels (K_{cl}) for the load shedding portion of the tests are plotted as a function of applied K_{max} in Fig. 3(a). It should be noted that closure levels are of the same order as generally observed for monolithic aluminum alloys (i.e. 1-2 MPam$^{1/2}$), and are typically much smaller than have been observed for other materials, e.g. steel and titanium alloys (Allison, 1988). There did not appear to be a significant effect of aging on closure stress intensity levels over the range of K_{max} studied.

It appears that over the range of applied K_{max} under investigation, K_{cl} is relatively constant. This type of behavior has previously been attributed to asperity-induced closure (Allison, 1988) (Fig. 3(b)). Evidence of asperity contact was clearly observed in crack profile examinations (Fig. 4). Oxide debris was also observed on the crack flanks close to threshold and, to a limited extent, on the fracture surfaces. The K_{cl} vs K_{max} behavior indicates, however, that the contribution of oxide-induced closure is probably dwarfed by the contribution from surface roughness. This is in agreement with results reported for IM 2xxx monolithic aluminum

alloys (Vasudevan and Suresh, 1982). Evidence for other possible crack tip shielding mechanisms (e.g. crack bridging and crack branching) are shown in Fig. 4(c),(d).

Fractography. A distinct difference in fracture surface morphology was observed to exist between near-threshold regions and regions associated with higher ΔKs.

Close to threshold, the fracture surfaces were generally much smoother than at high ΔKs, possibly due to fracture surface rubbing at very small crack tip opening displacements. In these threshold regions, the fracture surfaces showed the presence of particles which were analyzed as having strong silicon peaks. Matching-half fractography indicated that these particles were associated with like-sized voids (Fig. 5(a),(b)). This implies that near threshold SiC particles tend to decohere from the aluminum matrix.

At higher levels of ΔK, fracture surface observations show the presence of cracked SiC particles, similar to those previously observed for tensile fracture surfaces (You et al., 1987[2]). Evidence for the cracking of particles lies again in the examination of both fracture surfaces: particles on one half can readily be matched with their counterparts on the other half (Fig. 5(c),(d)). The incidence of these cracked SiC particles on the fracture surfaces appears to increase with increasing ΔK. This observation agrees well with reported fracture surface examinations on smooth fatigue specimens of similar composite material (VanDePolder and Jones, 1988).

The appearance of the overload fracture corresponds closely with that seen on monotonically loaded tensile specimens (Fig. 5(e),(f)), i.e. a combination of fractured and decohered SiC particles embedded in a dimpled aluminum matrix. As on the tensile fracture surfaces, it appears that cracked, or fractured, particles outnumber decohered particles.

CONCLUSIONS

1. The effect of matrix aging on fatigue crack growth behavior in a 2124-20%SiC_p composite was not pronounced. This was attributed to the fine grain size of the composite matrix.

2. The closure behavior indicated that asperity-induced closure was probably the dominant mechanism in these composites, although some evidence for limited oxide-induced closure was also present. Closure levels were not significantly influenced by aging treatment.

3. Differences in crack/microstructure interactions were observed as a function of ΔK. It was found that particle/matrix decohesion was prevalent at near-threshold ΔKs, with an increase in the incidence of particle cracking observed at higher levels of ΔK.

REFERENCES

J.E. Allison (1988). Fracture Mechanics: Eighteenth Symposium, ASTM-STP 945, 913-933.

P.E. Bretz, J.I. Petit, and A.K. Vasudevan (1984). Proc. Fatigue Crack Growth Threshold Concepts, 163-183, TMS Fall Meeting, Philadelphia, PA.

R.D. Carter, E.W. Lee, E.A. Starke, and C.J. Beevers (1984). Met. Trans., 15A, 555-563.

J.N. VanDePolder and J.W. Jones (1988). Presented at 1988 TMS Fall Meeting, Chicago.

A.K. Vasudevan and S.Suresh (1982). Met. Trans., 13A, 2271-2280.

A.K. Vasudevan and Bretz (1984). Proc. Fatigue Crack Growth Threshold Concepts, 25-42, TMS Fall Meeting, Philadelphia, PA.

C.P. You, A.W. Thompson, and I.M. Bernstein (1987)[1]. Presented at 116th TMS Annual Meeting, Denver. To be submitted to Met. Trans. for publication.

C.P. You, A.W. Thompson, and I.M. Bernstein (1987)[2]. Scripta Met., 21, 181-185.

C.P. You, J.V. Lasecki, J.M. Boileau, and J.E. Allison (1988). Presented at 1988 TMS Fall Meeting, Chicago.

E. Zaiken and R.O. Ritchie (1985). Mat. Sci. Eng., 70, 151-160.

M. Zedalis and M.E. Fine (1982). Scripta Met., 16, 1411-1414.

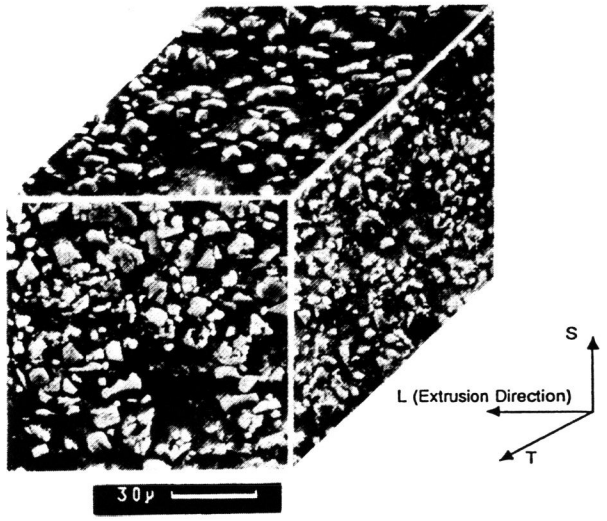

Fig. 1. Microstructure of 2124-20% SiC_p.

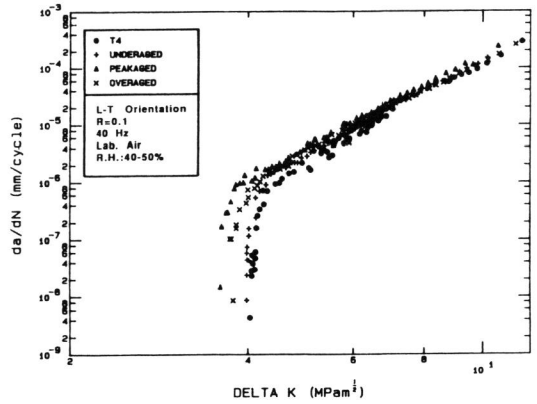

Fig. 2.
Variation of fatigue crack growth rate (da/dN) with applied stress intensity range (ΔK) for 2124-20% SiC_p in several aging conditions.

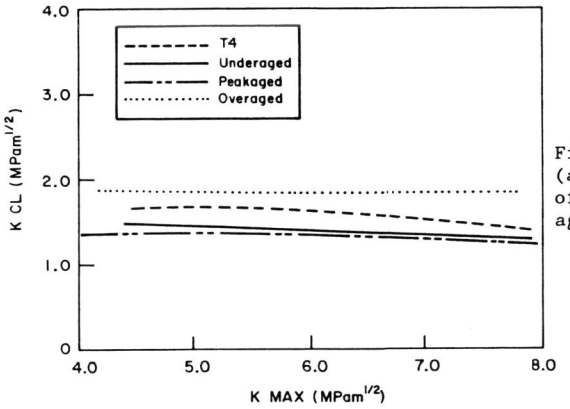

Fig. 3.
(a) Crack closure behavior of 2124-20%SiC_p for several aging conditions.

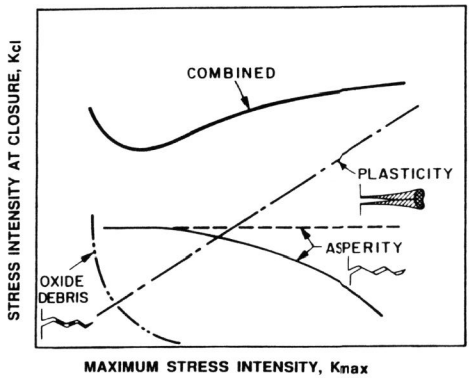

Fig. 3.
(b) Schematic indicating expected K_{cl} vs K_{max} behavior for three forms of crack closure, as well as their combined behavior.

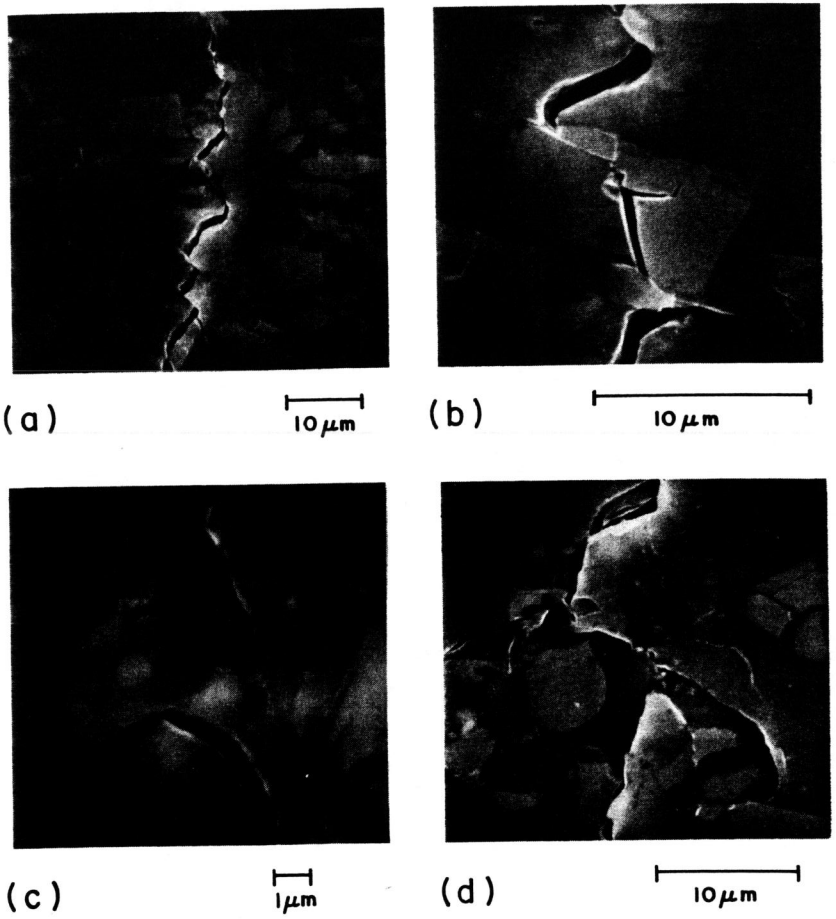

Fig. 4. SEM micrographs of crack profiles showing evidence of (a), (b) asperity-induced crack closure; (c) crack bridging; (d) crack branching.

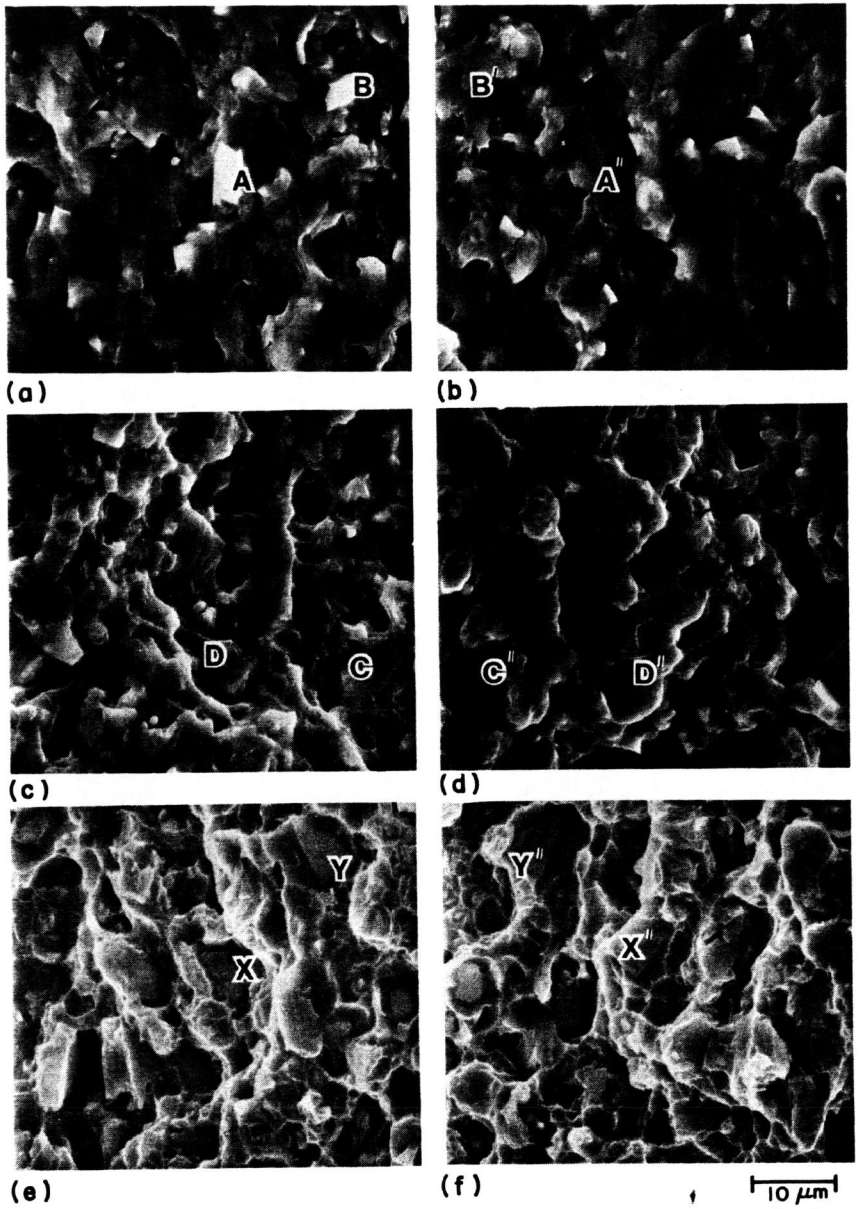

Fig. 5. Matching half fractography showing corresponding areas on both halves of the fracture: (a), (b) near-threshold region; (c), (d) ΔK=7 MPam$^{1/2}$ region; (e), (f) overload region.